ISBN: 978-3-95450-227-1 ISSN: 2673-5490 doi:10.18429/JACoW-IPAC2022-WEPOMS056

SPIN MATCHING AND MONTE-CARLO SIMULATION OF RADIATIVE SPIN DEPOLARIZATION IN e$^+$-e$^-$ STORAGE RINGS WITH BMAD*

O. Beznosov†, Los Alamos National Laboratory, Los Alamos, USA
J. A. Ellison, K. Heinemann, University of New Mexico, Albuquerque, USA
J. A. Crittenden, G. Hoffstaetter, D. Sagan, Cornell University (CLASSE), Ithaca, USA
D. P. Barber[1], DESY, Hamburg, Germany
[1] also University of New Mexico, Albuquerque, USA

Abstract

The *Bmad/Tao* software toolkit has been extended to estimate the rate of radiative spin depolarization in e^+-e^- storage rings. First estimates are made using the SLIM algorithm of linearized spin-orbit (s-o) motion. The extension implements the effects on s-o motion of stochastic photon emission using a Monte-Carlo tracking algorithm. Spins are tracked in 3-D along particle trajectories with the aid of Taylor expansions of quaternions provided by the Polymorphic Tracking Code (PTC). The efficiency of long-term tracking is guaranteed by the use of a sectioning technique that was exploited in previous-generation software (e.g. SLICKTRACK, SITROS). Sectioning is the construction of the deterministic s-o maps for sections between the dipoles during the initialization phase. Maps can be reused during the tracking. In a simulation for a realistic storage ring, the computational cost of initial map construction is amortized by the multi-turn tracking computational cost. The 1st-order terms in the quaternion expansions are used to construct the s-o coupling matrices in the matrices of the SLIM algorithm. These matrices are then available for an extension of the optimization facilities in *Bmad* to minimize depolarizing effects by spin matching.

INTRODUCTION

Relativistic electrons and positrons in storage rings emit synchrotron radiation and that can lead to a build up of spin polarization by the Sokolov-Ternov effect. At the same time noise is injected into the particle trajectories by the stochastic element of photon emission. The stochastic orbital variation couples via the T-BMT equation with the spin motion causing depolarization. The attainable equilibrium polarization results from the balance between the two effects. The rate of depolarization increases with beam energy much faster than the rate of polarization. Moreover the depolarization is enhanced near depolarizing resonances occurring when the closed-orbit spin tune ν_0 is close to an integer linear combination of the orbital tunes. See [1, 2] for details of these matters.

However it is highly desirable to have polarized beams at future high-energy rings like the proposed FCC-ee [3] and the CEPC [4, 5] as well as at the EIC [6] to extend the potential of the particle physics program as well as to provide a means of precise beam-energy calibration via resonant depolarization using radio-frequency transverse magnetic fields. Thus estimates of the attainable polarization are essential for guiding the design of a ring.

The attainable polarization can be estimated using perturbation theories to evaluate the terms in the Derbenev-Kondratenko (DK) formula [1, 2]. But the resulting formulas, describing the resonances, can be very complicated and the perturbation series might not converge. Moreover, at very high energy the so-called "uncorrelated resonance crossing" [7], whose effect is difficult to estimate with certainty, might dominate over the predictions of the DK formula. Thus it is better to rely on Monte-Carlo tracking simulations of the effects on spins of the magnetic and electric fields and of the stochastic photon emissions. An ideal modern framework for this is the *Bmad/Tao* software toolkit [8]. *Bmad/Tao* can handle nonlinear orbital motion, beam-beam forces and numerous phenomena in storage rings that go beyond standard spin-orbit tracking. Nevertheless, it always makes sense to begin with first-order perturbative analytical (SLIM) calculations to get a first impression of the situation. The SLIM formalism also provides structures for so-called spin matching, namely the method for minimizing depolarization at first order. This paper describes recent developments of *Bmad/Tao* spin simulation capabilities along with benchmarking with SLICKTRACK [1, 2].

RECENT DEVELOPMENTS IN BMAD/TAO SIMULATION TOOLKIT

Bmad/Tao has been extended to handle:

- Via the SLIM formalism [1, 2, 9] of linearized orbital and spin transport in terms of the 8×8 matrices which then can be analyzed using standard linear algebra techniques to deliver a first-order estimate of the rate of depolarization.
- Spin-orbit Monte-Carlo tracking with full 3-D spin motion implemented in a multi-turn/long-term tracking program which can employ many spin-orbit tracking backends: PTC [10], Bmad, One-turn Map, Multi-map with sectioning.
- Spin resonance strength calculations with energy scans implemented in a Python/PyTao script.

* Work supported by by the U.S. Department of Energy, Office of Science, Office of High Energy Physics, under Award Numbers DE-SC0018008 and DE-SC0018370
† obeznosov@lanl.gov

ISBN: 978-3-95450-227-1 ISSN: 2673-5490 doi:10.18429/JACoW-IPAC2022-WEPOMS056

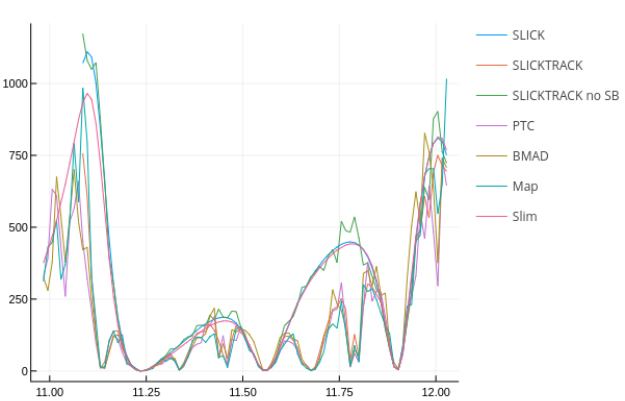

Figure 1: Depolarisation time (minutes) as a function of energy (GeV) computed using various spin-tracking and linear approximation codes for a test lattice. SLICK and SLIM curves display the results from linear codes. Others are results from tracking.

- *Bmad*-based program to convert *Bmad* lattices to SLICKTRACK format: *Bmad* lattice specifications are compatible with those of SLICKTRACK so that it can be used for testing and benchmarking future *Bmad* developments.
- Spin matching for minimizing depolarizing effects at first order in the SLIM framework while simultaneously maintaining functional optics and while being self-consistent with the *Bmad/Tao* spin-orbit tracking facilities.

The sectioning mentioned in the second item involves beginning a Monte-Carlo simulation by setting up and storing spin-orbit Taylor maps between the centers of dipole magnets and then subsequently using the pre-stored maps to transport spins and particles from dipole to dipole while radiating energy at each dipole. This results in a large increase in tracking speed compared to the speed available in element-by-element tracking.
In addition to SLIM, Monte-Carlo spin-tracking algorithms in *Bmad* were tested against SLICKTRACK results, see Fig. 1. For all test lattices after many improvements in both codes the comparison results are very good.

LINEARIZED SPIN-ORBIT MOTION (SLIM)

The SLIM formalism [1, 2, 9, 11, 12] has been implemented in *Bmad/Tao* since August 2018 [8]. We now briefly formulate the algorithm here and point out specifics associated with the *Bmad* implementation and refer the reader to the *Bmad* Manual [8] for more details.

The SLIM formalism expresses spin components using two right-hand coordinate systems

$$\big(\hat{l}(s), \hat{n}_0(s), \hat{m}(s)\big) \quad \text{and} \quad \big(\hat{l}_0(s), \hat{n}_0(s), \hat{m}_0(s)\big). \tag{1}$$

The axis $\hat{n}_0(s)$ is the unit-length, one-turn-periodic solution of the Thomas-BMT equation on the closed orbit. The axes $\hat{l}_0(s)$ and $\hat{m}_0(s)$ are unit-length solutions of the Thomas-BMT equation on the closed orbit and, generally, are not one-turn periodic. The axes $\hat{l}(s)$ and $\hat{m}(s)$ are chosen to be one-turn periodic but can have an arbitrary s dependence which can be chosen for convenience. The axes $\hat{l}_0(s)$ and $\hat{m}_0(s)$ are used for spin-matching and $\hat{l}(s)$ and $\hat{m}(s)$ are used for calculating polarization and depolarization. With respect to these axes, a unit-length spin $\mathbf{S}$ can be written as

$$\begin{aligned} \mathbf{S} &= \sqrt{1-\alpha_0^2-\beta_0^2}\,\hat{n}_0 + \alpha_0\,\hat{l}_0 + \beta_0\,\hat{m}_0, \quad \text{or} \\ \mathbf{S} &= \sqrt{1-\alpha^2-\beta^2}\,\hat{n}_0 + \alpha\,\hat{l} + \beta\,\hat{m}. \end{aligned} \tag{2}$$

At first order ($\alpha_0^2+\beta_0^2 << 1$ or $\alpha^2+\beta^2 << 1$) the spin component along $\hat{n}_0$ is a constant. With this, the eight-dimensional spin-orbit phase space used in the SLIM formalism is

$$(x, p_x, y, p_y, z, p_z, \alpha_0, \beta_0) \text{ or } (x, p_x, \ldots, p_z, \alpha, \beta). \tag{3}$$

where the orbital part $u = (x, p_x, \ldots, p_z)$ is taken with respect to the closed orbit.

The first-order map between any two points s_1 and s_2 is an 8×8 matrix $\widetilde{\mathbf{M}}$ which is written in the form

$$\widetilde{\mathbf{M}}(s_1, s_2) = \begin{pmatrix} \mathbf{M}_{6\times6} & \mathbf{0}_{6\times2} \\ \mathbf{G}_{2\times6} & \mathbf{D}_{2\times2} \end{pmatrix}, \tag{4}$$

where $\mathbf{M}(s_1, s_2)$ is the 6×6 orbital phase space transport matrix, and $\mathbf{G}(s_1, s_2)$ contains the coupling of the spin coordinates (α_0, β_0) or (α, β) to the orbital motion. The upper right block $\mathbf{0}_{6\times2}$ in the $\widetilde{\mathbf{M}}$ matrix is zero since Stern-Gerlach effects are ignored. When $\mathbf{G}$ is calculated with respect to the $(\hat{l}_0, \hat{m}_0)$ axes, large spin precessions on the closed orbit due to dipole and solenoid fields are eliminated. That leaves small precessions due to synchro-betatron motion. The $\mathbf{G}$ matrix then represents the dominating linear dependence of the small precessions on the six synchro-betatron coordinates and it then provides a good framework for analysis [1, 2, 13]. In Eq. (4), $\mathbf{D}$ is a 2×2 rotation matrix for the spin transport of a particle on the closed orbit. With $\hat{l}_0(s)$ and $\hat{m}_0(s)$ $\mathbf{D}$ is the unit matrix since they are solutions to the T-BMT equation. In contrast to the way how $\mathbf{G}$ and $\mathbf{D}$ are calculated in SLIM, *Bmad* calculates $\mathbf{G}$ and $\mathbf{D}$ from the first-order terms of Taylor expansions of quaternions, for spin-transport maps, provided by PTC.

Spin matching involves adjusting the optics and layout of a ring so as to minimise certain components of the $\mathbf{G}$ matrices, based on $\hat{l}_0(s)$ and $\hat{m}_0(s)$, for certain sections of a ring, thereby minimizing the influence of orbital motion on spin motion and minimizing the depolarization.

As shown in [1, 2, 9] to calculate of the rate of depolarization at this first order one needs the $\widetilde{\mathbf{M}}$ for one turn around the ring with a $\mathbf{G}$ based on α and β. Then the rate of depolarization can be obtained in terms of components of the eigenvectors of $\widetilde{\mathbf{M}}$.

ISBN: 978-3-95450-227-1 ISSN: 2673-5490 doi:10.18429/JACoW-IPAC2022-WEPOMS056

CALCULATION OF RESONANCE STRENGTHS

The **G** matrix, based on $\hat{l}_0(s)$ and $\hat{m}_0(s)$ can also be exploited to calculate the strengths of the resonances, ξ_r, needed to estimate the change of polarization, using the Froissart-Stora formula, when ν_0 changes as polarized electron or proton beams are accelerated through resonance conditions [14]. Thus

$$\xi_r = \frac{1}{2\pi}|(G(1,:) + iG(2,:))v_k|, \quad r = 1,2,3, \quad k = 2r-1,$$

where $G(1,:)$ and $G(2,:)$ are first and second rows of the G-matrix. In contrast to traditional treatments [15], this formalism handles fully coupled systems, giving resonance strengths for all three orbital modes at the correct orbital tunes for coupling. These resonance strengths also have a function in so-called harmonic synchro-beta spin matching for electrons (positrons) [1, 2]: reduction of resonance strengths can help to minimise depolarization.

These matters are illustrated in Fig. 2 which shows resonance strengths as a function of beam energy for the ATS and versions 5.2 and 5.3 of the ESR storage rings. The procedure for computing the resonance strengths for these lattices is as follows.

i) Begin with 14 GeV and 18 GeV lattices and

ii) Do an energy scan while varying the solenoid strengths so that the polarization is longitudinal at the IP, to find energies where ν_0 is in first-order resonance with an orbital tune.

iii) At each energy where there is a first-order resonance, vary the non-arc quadrupoles (except for quads near the IP in the region so that:

iv) The transfer matrices between solenoid pairs are decoupled and transfer matrices between the IP and the edges of the arcs regions are the same as the baseline lattice.

The lattice parameters for the test rings are shown Tab. 1.

Table 1: Lattice Parameters for Resonance Strength Scan

	ATS	ESR v5.2	ESR v5.3
Q_x	60.080765	49.119985	48.119983
Q_y	56.062995	43.099988	43.099988
Q_s	0.0442051	0.0442542	0.0444020
$a\gamma_0$	40.6265	40.4937	40.4937
Energy, GeV	17.902	17.8435	17.8435
ν_0	0.49962949	0.50017118	0.50017118
P_{ST}, %	90.66	82.78	81.16
P_{DKM}, %	73.08	65.02	61.79
P_x, %	85.94	74.63	70.81
P_y, %	90.67	82.78	81.16
P_s, %	73.862	64.02	58.96
τ_{BKS}, minutes	32.1	36.1	35.5
τ_{dep}, minutes	142	216	172

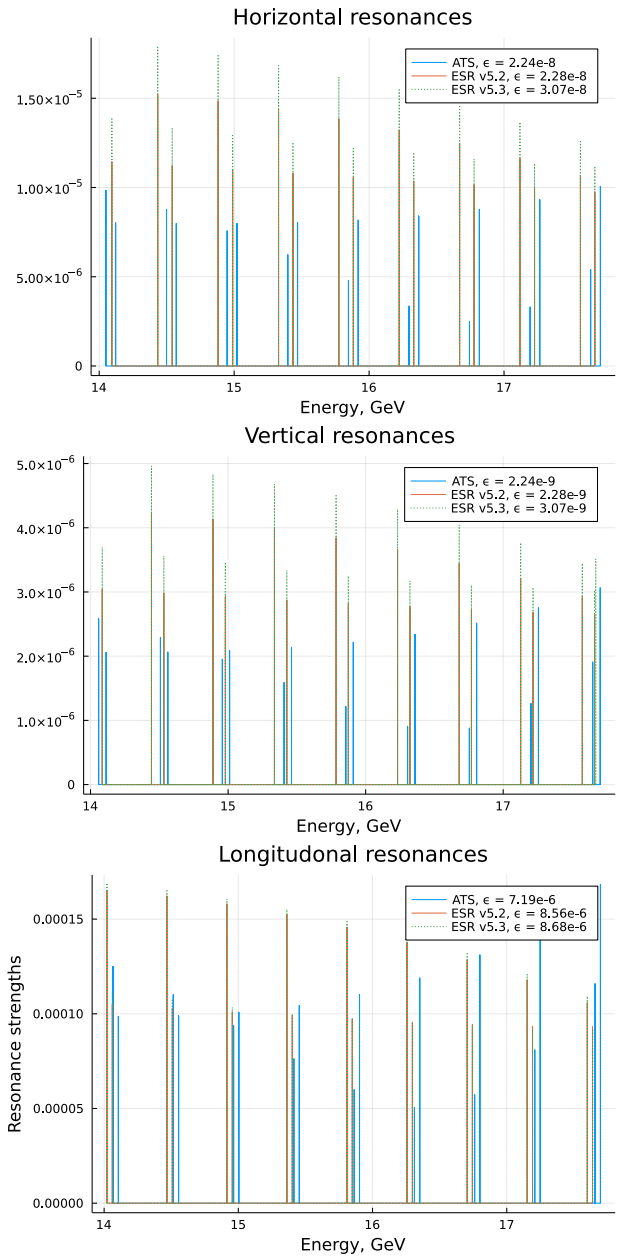

Figure 2: Resonance strength calculation.

CONCLUSION

The *Bmad/Tao* toolkit has been extended to become a powerful tool for Monte-Carlo simulations of depolarization in high-energy electron (positron) storage rings as well as to provide resonance strengths for fully coupled systems and spin matching and SLIM-like estimates self-consistently within the same package.

ACKNOWLEDGMENTS

This material is based upon work supported by the U.S. Department of Energy, Office of Science, Office of High Energy Physics, under Award Numbers DE-SC0018008 and DE-SC0018370.

ISBN: 978-3-95450-227-1 ISSN: 2673-5490 doi:10.18429/JACoW-IPAC2022-WEPOMS056

REFERENCES

[1] D. Barber and G. Ripken, "Radiative Polarization, Computer Algorithms and Spin Matching in Electron Storage Rings," in *Handbook of Accelerator Physics and Engineering*, 1st edition, 2006, pp. 174–182.

[2] D. Barber and G. Ripken, "Radiative Polarization, Computer Algorithms and Spin Matching in Electron Storage Rings," in *Handbook of Accelerator Physics and Engineering*, 3rd edition.

[3] A. Abada *et al.*, "FCC-ee: the lepton collider," *The European Physical Journal Special Topics*, vol. 228, no. 2, pp. 261–623, 2019.

[4] CEPC Accelerator Study Group, *Snowmass2021 white paper af3-cepc*, 2022, doi:10.48550/ARXIV.2203.09451

[5] The CEPC Study Group, *Cepc conceptual design report: Volume 1 - accelerator*, 2018, doi:10.48550/ARXIV.1809.00285

[6] BNL, *Electron–Ion Collider*, https://www.bnl.gov/EIC, Accessed on 2022-06-06, 2012.

[7] Y. S. Derbenev, A. M. Kondratenko, and A. N. Skrinsky, "Radiative polarization at ultrahigh-energies," *Part. Accel.*, vol. 9, pp. 247–266, 1979.

[8] D. Sagan, *The BMAD Reference Manual*, Revision: May 13, 2022.

[9] A. W. Chao, "Evaluation of radiative spin polarization in an electron storage ring," *Nuclear Instruments and Methods*, vol. 180, no. 1, pp. 29–36, 1981.

[10] E. Forest, F. Schmidt, and E. McIntosh, "Introduction to the polymorphic tracking code," *KEK report*, vol. 3, p. 2002, 2002.

[11] A. W. Chao, "Evaluation of beam distribution parameters in an electron storage ring," *Journal of Applied Physics*, vol. 50, no. 2, pp. 595–598, 1979.

[12] J. A. Ellison, K. Heinemann, and H. Mais, "Orbital Eigen-Analysis for Electron Storage Rings," in *Handbook of Accelerator Physics and Engineering*, 3rd edition.

[13] D. P. Barber, J. Kewisch, G. Ripken, R. Rossmanith, and R. Schmidt, "A solenoid spin rotator for large electron storage rings," *Part. Accel.*, vol. 17, p. 243, 1984, DESY-84-102.

[14] G. H. Hoffstaetter, *High energy polarized proton beams: a modern view*. Springer, 2009, vol. 218.

[15] E. Courant and R. Ruth, "BNL report," *BNL-51270*, 1980.